NeuroImage 196 (2019) 173–187

Contents lists available at ScienceDirect

NeuroImage

journal homepage: www.elsevier.com/locate/neuroimage

Normative event-related potentials from sensory and cognitive tasks reveal occipital and frontal activities prior and following visual events

F. Di Russo [a,*], Berchicci M [a], Bianco V [b], Perri RL [a,c], Pitzalis S [a,b], Quinzi F [a,b], Spinelli D [a]

[a] Dept. of Movement, Human and Health Sciences, University of Rome "Foro Italico", Rome, Italy
[b] Santa Lucia Foundation (IRCCS Fondazione Santa Lucia), Rome, Italy
[c] University of Rome Niccolò Cusano, Italy

A B S T R A C T

In the present study, we report the results from a large sample of participants (N = 136), selected based on their EEG quality, to obtain event-related potential (ERP) normative data. All participants were tested in Simple Response Task (SRT) and Discriminative Response Task (DRT). A subset of 36 participants was tested also in Passive Vision task. Both pre- and post-stimulus ERPs were analyzed and compared among different tasks. Spatiotemporal patterns of all the observed components were analyzed using source analysis. Beside the well-known ERP components, we also described recently identified prefrontal components: the pre-stimulus prefrontal negativity (pN) associated to proactive cognitive (mainly inhibitory) control within the inferior frontal gyrus (iFg); the post-stimulus prefrontal N1, P1 and P2 (pN1, pP1 and pP2) involved in perceptual and visual-motor awareness (pN1 and pP1), and in stimulus-response mapping and decision-making (pP2) localized within the insular cortex. The large sample of high-quality EEG datasets allowed to identify four additional components: the pre-stimulus visual negativity (vN) originating in extrastriate visual areas and interpreted as a visual readiness activity; the post-stimulus prefrontal N2 and N3 (pN2 and pN3) components interpreted as feedback reactivation of the anterior insular cortex; and the post-stimulus prefrontal P3 (pP3), interpreted as persisting inhibitory activity of the iFg for inhibited trials.

1. Introduction

Event-related potentials (ERPs) represent a pivotal research method in cognitive neuroscience. By measuring brain electrical activity with high temporal resolution, ERPs allow to capture and segregate fast and complex dynamics of neural processing. Despite ERPs have been studied for over 50 years, it is fascinating to note that new components and functional aspects can still be identified nowadays. The present study will introduce some novel components (both pre- and post-stimulus) and, due to the availability of a large sample, will provide normative data for both canonical and novel components.

In the last few years, research fostered the existence of some prefrontal ERP components related to cognitive processing in tasks requiring motor responses (or inhibition) to visual stimuli. These prefrontal components could be not variants of old components, since they involve cortical regions that have never been reported before; further, although detected in the specific context of visuomotor tasks, these components hold general interest, especially for challenging cognitive processing of daily lives (see Di Russo et al., 2017 for review). For instance, Go/No-go discriminative response tasks (DRTs) may activate processes similar to those taking place in everyday life when we select an action in response to a visual stimulus and refrain from acting to another stimulus (the easiest example is our behavior with green/red traffic light). In general, the Go/No-go paradigm may mimic very frequent processing of human goal-directed behavior, although a crucial difference between everyday life and experimental context is that the same event and task is replicated hundreds of time in laboratory studies, in order to average reliable electrical response.

1.1. Pre-stimulus components

In the Go/No-go DRT, a novel slow negative anticipatory wave was recently identified over prefrontal sites, starting well before (i.e. 800 ms) the occurrence of a visual event and named prefrontal negativity (pN) (Berchicci et al., 2012; Kamijo et al., 2016; Gonçalves et al., 2018). The pN source has been localized in the pars opercularis of the inferior frontal gyrus (iFg) and the component has been associated with proactive cognitive functions (Di Russo et al., 2016; Sulpizio et al., 2017; Berchicci et al., 2018), especially inhibition (Bianco et al., 2017b). Thus, this novel pN component adds to the family of preparatory slow components, and the present large dataset will show its correlation with behavioral data.

ERP literature on action preparation mainly focused on the Bereitschaftspotential (BP) in self-paced motor tasks (Kornhuber and Deecke, 1965) with cortical a source in the supplementary and cingulate motor areas (SMA and CMA). In self-paced tasks the BP peaks over medial frontal electrodes (e.g. Shibasaki and Hallett, 2006); in externally-triggered tasks, functional magnetic resonance (fMRI) studies

* Corresponding author.
E-mail address: francesco.dirusso@uniroma4.it (F. Di Russo).

https://doi.org/10.1016/j.neuroimage.2019.04.033
Received 19 March 2019; Received in revised form 7 April 2019; Accepted 8 April 2019
Available online 11 April 2019

Acronyms

pN	(prefrontal Negativity)
vN	(visual Negativity)
BP	(Bereitschaftspotential)
pN1	(prefrontal N1)
pN2	(prefrontal N2)
pN3	(prefrontal N3)
pP2	(prefrontal P2)
dpP2	(differential pP2)
SMA	(Supplementary Motor Area)
CMA	(Cingulate Motor Area)
iFg	(inferior Frontal gyrus)
aIns	(anterior Insula)
aIPs	(anterior Inferior Parietal sulcus)
SRT	(Simple Response Task)
DRT	(Discriminative Response Task)

reported similar premotor sources (Cunnington et al., 2002, 2003; Di Russo et al., 2016), but in ERP studies with SRT and DRT a more posterior scalp distribution was reported (Di Russo et al., 2016, 2017; Bianco et al., 2017a,c).The present study will propose an explanation for this posterior topography.

In previous studies (Di Russo et al., 2016; Bianco et al., 2017b) we suggested that the BP and the pN might reflect a sort of proactive *accelerator/brake system* that, based on predictive internal models, plans and anticipates future actions. In line with this view, the present study will confirm that the BP amplitude predicts response times and it will show that in DRT the pN amplitude (especially on the right side) is related to the percentage of errors.

It is noteworthy to point out that, compared to contingent negative variation (CNV) and stimulus-preceding negativity (SPN) tasks generally used to study anticipatory processing, the DRTs (as used in the present study) have fewer confounding factors due to the absence of task-related cues and response feedback. This might allow to better capture undetected or masked activities. In particular, DRTs are based on target and non-target sequences, administered with a variable inter-stimulus interval. Although different protocols may induce similar brain activities during the preparation phase, some ERP activities appear to be distinctive of the selected task: for example, the pN component described in DRTs seems characteristic of this task, since pN-like components have never been reported in CNV and SPN studies (for a discussion on this point, see Di Russo et al., 2016).

1.2. Anticipation of visual events

The main goal of predictive models is to optimize performance; in particular, Bayesian models of cognition (e.g. Griffiths et al., 2008; Jones and Love, 2011) propose the existence of cerebral processes underlying perceptual anticipation of upcoming events. Relevant for the present study, a clear ERP component related to *anticipation of sensory events* has never been reported. However, fMRI studies (e.g. Kastner et al., 1999) showed activation of striate and extrastriate cortices during the fore period of attended visual stimuli, and electroencephalographic studies described pre-stimulus frequency synchronization/desynchronization (e.g., Brunia and Van Boxtel, 2004). With ERPs, a slow-wave activity was found at occipital level modulated by expectancy of self-administered emotional pictures (Perri et al., 2014a); further, regarding to non-self-paced conditions, ERP investigations describing CNV and SPN showed posterior areas activities in complex tasks involving predictive cues and response feedback, respectively (Brunia et al., 2011; Gómez et al., 2003; Gómez et al., 2007; Brunia and Van Boxtel, 2004; van Boxtel and Böcker, 2004). Thus, there is some support to the hypothesis that an ERP component related to anticipation of visual events can be found in visual-motor tasks. The present study will provide evidence in favour of this view.

More specifically, we started our investigation with the aim to explain the BP "posteriorization" which we observed in various previous studies during the preparation of externally-triggered visual-motor tasks (Di Russo et al., 2016, 2017; Berchicci et al., 2018; Bianco et al., 2017a,c). We supposed that this posteriorization might be explained by the contribution of occipital sensory areas, actively involved in the anticipation of upcoming visual stimulus (Knill and Richards, 1996; Mamassian et al., 2002), which add up on the scalp to the electrical fields from the premotor areas. To this end, we considered a passive viewing task as a control condition since it allows to exclude possible confounding factors due to motor preparation activities.

Passive viewing also allows evaluating whether occipital activity reported by some CNV and SPN studies was task-specific (such as attention to the cue and to the feedback in CNV and SPN, respectively) or reflected a default process of stimulus expectancy that is present also in passive vision. In this latter case, the occipital activity would reflect the readiness of the visual areas, independent from the motor demand and the content of the visual stimuli (e.g., cues and feedback for CNV and SPN, respectively). The present large sample will provide a reliable answer to the question of anticipatory activity of sensory events.

1.3. Post-stimulus components

ERPs literature on anticipatory phase is relatively small compared to the impressive amount of contributions on post-stimulus ERPs (e.g. Luck and Kappenman, 2011; Luck, 2014). However, despite the introduction of many tasks and signal analysis techniques, some post-stimulus ERP components have been neglected so far. Recently, we described peculiar components possibly originating from the anterior insular cortex (e.g. Di Russo et al., 2016), paving the way for innovative investigation of anterior lobes by means of ERPs. These components, labelled as prefrontal N1 (pN1), P1 (pP1) and P2 (pP2), peak over prefrontal sites at around 110 ms, 180 ms and 300 ms respectively. The pN1 and the pP1 have been associated with visual and visual-motor awareness, while the pP2 has been linked to response-related processing of sensory evidence accumulation when decision-making is required (Berchicci et al., 2016; Di Russo et al., 2016; Gonçalves et al., 2018; Perri et al., 2018a,b,2019; Potts et al., 1996; Sanchez-Lopez et al., 2017; Ragazzoni et al., 2019; Sulpizio et al., 2017). The pN1 and the pP1 are modulated by visuospatial attention (Berchicci et al., 2019). The pP2 can be assimilated to other components independently described for different tasks (e.g. Perri et al., 2017, 2018a; Potts et al., 1996), but it is a different component with respect to the P3a evoked by novel, unattended stimuli for several features: 1) the P3a scalp topography is medial and central (usually measured at Cz, e.g. Polich, 2007), while the pP2 is more anterior showing a bilateral prefrontal distribution (usually peaking at AF7/AF8 or Fp1/2.2) The P3a is evoked by unexpected stimuli not requiring response, while the pP2 is evoked by target stimuli. 3) The functional significance of the P3a has been linked to orientation and attention processes stemming from a working memory representational change (e.g. Polich, 2007), while the pP2 has been related to decisional processes in stimulus/response mapping (e.g. Perri et al., 2017). 4) The P3a has been localized in the hippocampus, in the anterior cingulate cortex and other structures associated with the salience network (e.g. Polich, 2007), while the pP2 has been localized in bilateral anterior insula (Di Russo et al., 2016; Ragazzoni et al., 2019; Sulpizio et al., 2017). The salience network also includes the anterior insula, but the insular activity does not seem to directly contribute to the P3a generation (Menon and Uddin, 2010). It is noteworthy to point out that the pN1 and the pP1 components can be detected in any visuomotor task, including simple response tasks (SRT), while the pP2 is specific for tasks involving decisional processes such as stimulus categorization in DRTs. In conclusion, the novel abovementioned prefrontal pre- and post-stimulus components have

been reported in a limited number of studies and, at present, no normative data exist. The main aim of the present work is to provide normative ERP data on these recently discovered prefrontal components (both pre- and post-stimulus) using a large sample of adults with high-quality (stable and very low-noise level) EEG signal in SRT and DRT. Moreover, in a subgroup of participants tested also in a passive viewing condition, we aimed to describe the contribution of occipital areas in the pre-stimulus stage and to evaluate whether these were active in the anticipation of upcoming visual stimulus in both purely visual and visuomotor tasks.

Normative data in tasks involving a sequence of stages -including preparation, perception, discrimination, decision and action may provide a reliable reference for electrophysiological research on cognitive processing in visuomotor tasks useful for both healthy subjects and patients. Note that the tasks that are taken into account here (passive vision, simple detection and discriminative responses) are frequently used in the literature; with the purpose to simplify the comparison to existent literature, we analyzed ERP on scalp locations available in low-resolution EEG montage.

2. Methods

2.1. Participants

Participants were selected from a large database of EEG data with more than 400 subjects performing the visuomotor tasks described below. The dataset has been built up by the "Cognitive and Action Neuroscience Lab" of the University of Rome "Foro Italico" during the last 15 years and contains EEG of healthy participants and patients ranging from 6 to 89 years. For the present study, the inclusion criteria of individuals were the following: 1) Healthy adults (no history of neurological, psychiatric, or chronic somatic disease) from 18 to 45 years of age; 2) High-quality EEG signal, that is activity not contaminated by considerable electrooculographic (EOG) and electromyographic (EMG) artifacts defined as amplitude not exceeding ±70 μV for more than 10% of recording time. The sample was gender-matched. Based on this selection, 100 participants met the inclusion criteria. Moreover, we recruited additional participants to test them in a passive vision task and in the same visumotor tasks used in the main group; 36 participants met the inclusion criteria. Overall, 136 subjects participated to the study (68 females) with a mean age of 30.5 ± 9.4 yrs (range 18–45 yrs). In the passive task (18 females) the mean age of the group was comparable to that of the whole group (29.7 ± 7.2 yrs, range 20–42 yrs).

All participants reported that they were not taking psychoactive or vasoactive medication and had normal or corrected-to-normal vision. All participants were right-handed (Edinburgh handedness inventory, Oldfield, 1971). The participants' written informed consent was obtained according to the Declaration of Helsinki after approval by the ethical committee of the IRCCS Santa Lucia Foundation.

2.2. Stimuli and task design

Each participant was tested in a sound-attenuated dimly lit room after the EEG cap was mounted on the scalp. They comfortably seated in front of a 24" computer screen at a distance of 114 cm with a response button pad positioned under their right index finger. In the screen center, a fixation point was present (0.15° diameter circle) that never disappeared. Four visual stimuli (i.e. squared configurations subtending 4 × 4° and made by vertical and/or horizontal bars) were randomly displayed for 250 ms with equal probability ($p = 0.25$); the stimulus-onset asynchrony varied from 1 to 2 s to prevent stimulus prediction and ERP overlaps with previous and following stimuli. All participants performed two tasks: 1) a visuomotor simple response task (SRT), in which they had to respond as soon as possible to any stimulus; 2) a discriminative response task (DRT) in which they had either to press the button as soon as possible only when (two out of four) designed target stimuli appeared on the screen ($p = 0.5$), or to withhold the motor response when non-target stimuli appeared ($p = 0.5$); in DRT speed and accuracy performance were equally emphasized by instructions.

A subgroup of 36 participants performed also a third task requiring passive vision of the four stimuli above described with the same stimulus presentation timing. Compared to SRT and DRT, the only difference was that no response was required in this passive vision task (from now on, Passive task, or Passive). Graphic representation of the paradigms is shown in Fig. 1. The presentation order of the four stimuli was randomized. The number of trials for any task (Passive, SRT, DRT target and DRT non-target) ranged from 340 to 440. The duration of each run was approximately 2.5 min; the Passive task and the SRT lasted about 15 min each, while the DRT about 25–30 min, depending on the individual rest time between trials. The order of the tasks was counterbalanced across participants.

2.3. Behavioral data

In SRT and DRT, the response speed was calculated using the median RT for correct trials at the individual level (because less skewed than the mean), whereas the mean value of the RT was considered at the group level. To evaluate response consistency, individual mean RT and its standard deviation (SD) were used to calculate the intra-individual coefficient of variation (ICV= SD/mean RT). Accuracy was assessed considering both the percentage of omission errors (OE, i.e., missing responses to targets) and the percentage of commission errors (CE, i.e., responses to non-targets, limited to DRT). The OE in the SRT was not reported because nearly absent (less than 1%).

2.4. EEG data recording and analysis

Since the EEG database was acquired in an extended timeframe, two

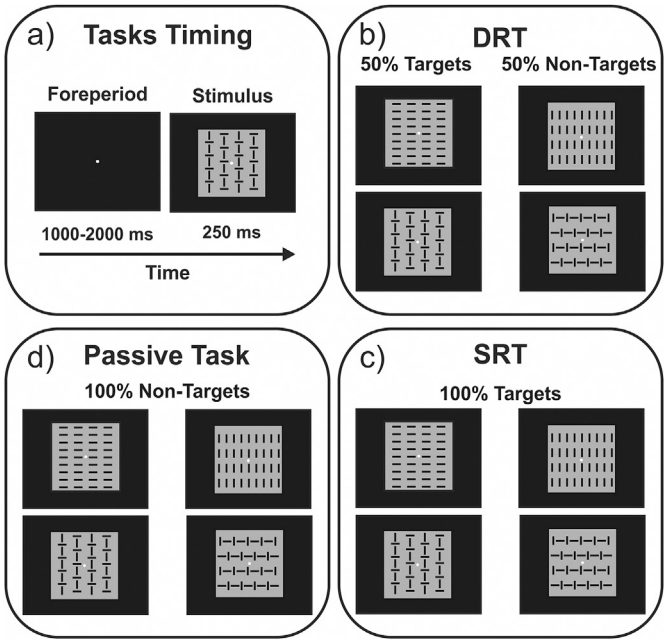

Fig. 1. Schematic representation of the three tasks considered in the study. a) The figure shows the timing characteristics common to all tasks. On the left side, during the fore-period ranging between 1 and 2 s, only the fixation point was displayed; on the right side, one of the four possible patterns is shown, superimposed for 250 ms over the fixation point. b) In the discriminative response task (DRT) 50% of the stimuli were targets (left side) requiring a motor response, the other 50% were non-targets (right side). c) In the simple response task (SRT) all stimuli were targets, always requiring a motor response. d) In the passive task, all stimuli were non-targets, not requiring responses.

setups were used, contingent on the acquisition of new instruments. For 67 participants, the EEG was recorded using two standard BrainAmp™ amplifiers (BrainProducts, Germany) system with 64 electrodes (setup 1). Two of these electrodes were used to monitor EOG with bipolar montage. Horizontal EOG (HEOG) was recorded between one electrode placed on the right eye canthus and a second electrode placed below the left eye. Vertical EOG (VEOG) was recorded between below the left eye and Fp1 (setup 1). For the remaining 69 participants, a third BrainAmp™ amplifier (ExG type) was used to record EOG with four electrodes configured in two bipolar pair: one pair of electrodes placed on the left and right canthi (HEOG), and the second pair placed below and above the left eye (VEOG). This montage (setup 2) allowed to record the EEG from 64 channels, and 4 EOG channels. For both setups, Ag/AgCl sintered electrodes were used. EEG channels were placed according to the 10-10 International system, initially referenced to the M1 and, then, off-line re-referenced to the M1-M2 average. Setup 1 included more posterior electrodes: Inion (I7, I3, I4 and I6) and sub-Inion (SI3, SIz and SI4), parietal-occipital (PO9 and PO10) and parietal (P9 and P10). Setup 2 covered more anterior sites, including all frontopolar (Fpz), anterior-frontal (AF9, AF5, AF3, AF2, AF4 and AF10) and frontal (F9, F1, F2, F10) electrodes. Merged together, these two setups allowed a grand-averaged ERP based on 88 EEG channels. Most of these 88 channels (52) were common to both setups, while the remaining channels (36) were present only in a subgroup of 63 and 69 subjects for SRT and DRT, respectively. Only common channels were used for statistical analysis, whereas all of them were used to show comprehensive scalp topographies and source localization. For both setups, EEG was digitized at 250 Hz, amplified (bandpass of 0.01–60 Hz including a 50 Hz notch filter) and stored for offline averaging. Data were recorded and analyzed using the Recorder 1.21 and the Analyzer 2.11 software (BrainProducts, Germany). Removal of ocular artifacts was performed using independent component analysis (ICA) on the raw EEG (e.g. Jung et al., 2000). Further, artifact rejection was performed prior to signal averaging to discard epochs still contaminated by signal exceeding the amplitude threshold of ±50 μV. Less than 5% of the trials was rejected. Continuous EEG was segmented in epochs starting 1100 ms prior to the stimulus onset and lasting for 2000 ms, and separately averaged for each condition (Passive task, SRT, DRT target and DRT non-target). Since trials were equally and randomly presented in the task, pre-stimulus ERPs in the DRT were obtained averaging both target and non-target trials. In all conditions, the pre-stimulus components amplitude was measured with a −1100/-900 ms baseline; the post-stimulus components amplitude was calculated with respect to −200/0 ms baseline. The components latency was taken as the latency of peak amplitude. Trials with OEs and CEs were excluded from the ERP averages.

2.5. Sources analyses

Source analyses were performed on individual ERPs after re-refencing to averaged reference. The spatiotemporal module of the BESA research 6.1 system and BESA statistics 2.0 (MEGIS, Germany) software was used for neural source localization of the detected components, 3D scalp mapping and statistics. The BESA has the advance to either fit or seed equivalent electrical dipole in specific brain locations and obtain for each them the relative time-course (dipole moment) of specific brain areas and compare them with the scalp waveforms. BESA allows creating either data-driven ERP source models or models based on previous knowledge as neuroimaging data. In the present study, five independent models were obtained: An initial un-seeded model (both dipole locations and orientation were fitted on ERP data only) was obtained for the passive task. Then four other models were seeded in the brain locations found in previous fMRI studies (Di Russo et al., 2016; Sulpizio et al., 2017) using a similar DRT, and orientations were fitted on ERP data from the four studied task conditions (Passive, SRT, DRT target and DRT non-target). Each source model was first fitted on the grand-average ERP to obtain a stable model, which was then optimized on each individual ERP. Then, the individual source locations, orientations and time-courses were averaged to obtain the final model and used for statistical comparison as *t*-test again zero to test the dipole time course trustworthiness. See results for more details.

Additional source analysis was performed using a data-driven distributed method on individual ERP in the passive viewing task in order to confirm BESA result. We used the "exact low-resolution brain electromagnetic tomography" (eLORETA) software (freely available at www.uzh.ch/keyinst/loreta.htm) to compute the cortical three-dimensional distribution of the ERP current density. eLORETA has no localization bias, even in the presence of structured noise, and, in this sense, it is an improvement over LORETA (Pascual-Marqui et al., 1994) and the standardized version sLORETA (Pascual-Marqui, 2002).

2.6. Statistical analysis

For behavioral data, the RT and the ICV were submitted to analysis of covariance (ANCOVA) comparing the DRT with the SRT, including age as a covariate to control for possible adult developmental changes in the considered age range (18–45 yrs).

Considering the absence of peak activities, the pre-stimulus ERP interval, the mean activity from the ERP onset (−800 ms) to stimulus appearance (time zero) was used for statistical analyses.

The amplitude of post-stimulus ERP components were analyzed considering the mean activity of short intervals (from ±50 ms to ±100 ms) around the peak amplitude, more specifically in the following epochs and electrodes: the P1 and the N1 between 100 and 200 ms at lateral occipital and parieto-occipital electrodes; the pN1 and the pP1 in the same interval, but at medial and lateral prefrontal channels; the pP2 between 200 and 400 ms at medial prefrontal channels; the P3 between 250 and 350 ms in the SRT and from 400 to 600 in the DRT at medial central and central-parietal electrodes (for a review on features and functional interpretation of these ERP components, see Di Russo et al., 2017). Except for the non-target pP2, which did not show a clear peak, the other components had clearly detectable peaks in the 92–97% of individual ERPs.

Repeated measure analysis of variance (ANOVA) implemented in the BESA statistics 2.0 was used the evaluate effects and interactions among conditions in the region of interest (ROI) where peak activity of each component was detected. For the pre-stimulus ERP, the pN amplitude was submitted to a 3×2 ANOVA with 3 conditions (DRT, SRT and Passive) and 2 ROIs, according to the bilateral prefrontal scalp topography of this component. The left ROI pooled Fp1, AF3 and AF7 electrodes and the right ROI pooled Fp2, AF4 and AF8 electrodes. The BP amplitude was submitted to a one-way ANOVA with 3 Conditions (DRT, SRT and Passive). Being the BP topography medial, the used ROIs pooled Cz and CPz electrodes. The use of bilateral prefrontal ROIs for the pN was also motivated by literature on the right prefrontal cortex dominance in the inhibitory control (e.g. Aron et al., 2004).

For the post-stimulus ERP, repeated measure ANOVAs were performed on the P1 and the N1 using a 4×2 design with 4 Conditions (DRT target, DRT non-target, SRT and Passive) and 2 ROIs (PO7 and PO8). The pN1 and the pP1 were analyzed using a 4-way ANOVA (conditions) at the AFz ROI. The pP2, the N2 and the P3 were present in the DRT only and analyzed using a 2×2 ANOVA with 2 Conditions (target and non-target) and 2 ROIs (AF7 and AF8 for the pP2; Fz and Cz for the N2; Cz and CPz for the P3). The other components were not analyzed by means of ANOVAs, because not visible in all conditions (as the C1, P2, pN2-3 and pP3). The use of bilateral or medial ROIs was motivated by the scalp distribution of the studied component.

In addition, Pearson's correlations were computed between the ERP components amplitude or latency and behavioral data; results were adjusted using the Bonferroni correction for multiple comparisons based on 52 electrodes. Scheffe's post-hoc test was used for multiple comparisons correction. Scheffe's test is recommended for ERP analysis (e.g. Luck and Gaspelin, 2017), because it computes F-values for all pairwise

comparisons of groups/conditions and determines a new critical F-value indicating which individual pairwise comparisons of groups/conditions are significant. Alpha level was set at 0.05 for all statistical analyses.

The ERP component names used in the present work follow the successive deflection nomenclature (i.e. P1, P2, P3) recommended by Luck and Kappenman (2011) and generally used in cognitive tasks, instead of the nominal latency nomenclature (i.e. P100, P200, P300), which is more common in clinical studies (e.g. Hari and Puce, 2017; Pernet et al., 2018).

Present data will be made available on request in compliance with the requirements of the funding institutes, and with the institutional ethics approval.

3. Results

3.1. Behavioral data

For the SRT the mean response time was 222 ms (SD = 24) and for the DRT 442 ms (SD = 51). The ICV was 0.170 (SD = 0.036) and 0.184 (SD = 0.042) in SRT and DRT, respectively. In the DRT the Omission errors were 2.0% (SD = 1.8) and the Commission errors were 8.9% (SD = 6.4). Statistical comparisons between tasks showed that RT in the DRT was slower ($F_{(2,134)} = 386.7$, $p < 0.0001$, $_p\eta^2 = 0.87$) than in the SRT. The effect of age ($F_{(1,134)} = 2.4$, $p = 0.13$, $_p\eta^2 = 0.02$) and the interaction ($F_{(1,134)} = 2.2$, $p = 0.12$, $_p\eta^2 = 0.02$) were not significant. Regarding the ICV, the RT was more variable ($F_{(2,134)} = 251.1$, $p < 0.0001$, $_p\eta^2 = 0.85$) in the DRT than in the SRT. The effect of age ($F_{(1,134)} = 2.7$, $p = 0.11$, $_p\eta^2 = 0.03$) and the interaction ($F_{(1,134)} = 2.8$, $p = 0.10$, $_p\eta^2 = 0.03$) were not significant.

3.2. Pre-stimulus ERP

Fig. 2 shows pre-stimulus ERPs temporal evolution (Fig. 2a) and spatial topography (Fig. 2b). In DRT, the pN is the first detectable activity starting from −800 ms on bilateral prefrontal electrodes and emerging as slow-rising negativity reaching the climax just before stimulus onset. The pN topography showed a bilateral prefrontal distribution in the early phase (−800/-500 ms) and a medial prefrontal distribution in the later phase (−500/0 ms). The BP emerged at −750 ms and, similarly to the pN, raised slowly but with a higher slope than the pN. The BP focused on medial central-parietal scalp during the whole pre-stimulus period and peaked after stimulus onset. In SRT, the pN was not clearly detectable, even though not totally absent, while the BP emerged at −800 ms, which is a bit earlier and with a slower slope than in DRT; however, their topographies were similar in the −500/0 ms interval.

As stated in the introduction, the BP originates in SMA and CMA, but the present posterior distribution seems to contrast with the expected activity of these frontal regions. The explanation for these apparently inconsistent results can be found in the observation of the pre-stimulus activity in the Passive task. This passive viewing condition allows the identification of a bilateral activity at parietal-occipital sites (Fig. 2b, right side; for similar results see Perri et al., 2018b). This component, hereinafter referred to as visual negativity (vN), started at −850 ms with an initial steep slope that then reduced, and peaked concomitantly to stimulus onset at PO7 and PO8 electrodes. The vN emerged clearly in the Passive task because it was the only detectable activity before stimulus onset; however, once its spatiotemporal profile is well characterized, the vN can be detected also in the SRT and, with lower amplitude, in the DRT as well (see PO7 and PO8 electrodes in Fig. 2a). Table 1 shows the mean amplitude of the studied components.

Fig. 3 shows comparisons (by differential waves) between pre-stimulus ERPs obtained in the three tasks in terms of temporal evolution (Fig. 3a) and spatial topography (Fig. 3b). Comparing DRT and SRT, differences were present at both occipital and prefrontal level, the vN peaked at −700 ms and then remained steadily high up to few milliseconds after stimulus onset. The DRT minus Passive task subtraction confirmed the pN and vN differences; in addition, the BP component was present in DRT only. It is important to note that in DRT minus Passive (differential) map (Fig. 3b, middle), the distribution was more anterior than in DRT topography (Fig. 2b, left side bottom). The differential topography is like the frontal BP topography usually found before self-paced movements (e.g. Jahanshahi and Hallett, 2003). It is likely that the vN activity in DRT produced an overall posterior shift of the BP topography with respect to self-paced movement topography (where no visual stimulus is presented). Lastly, comparing SRT and Passive task, the only difference was due to the BP that was present in SRT only.

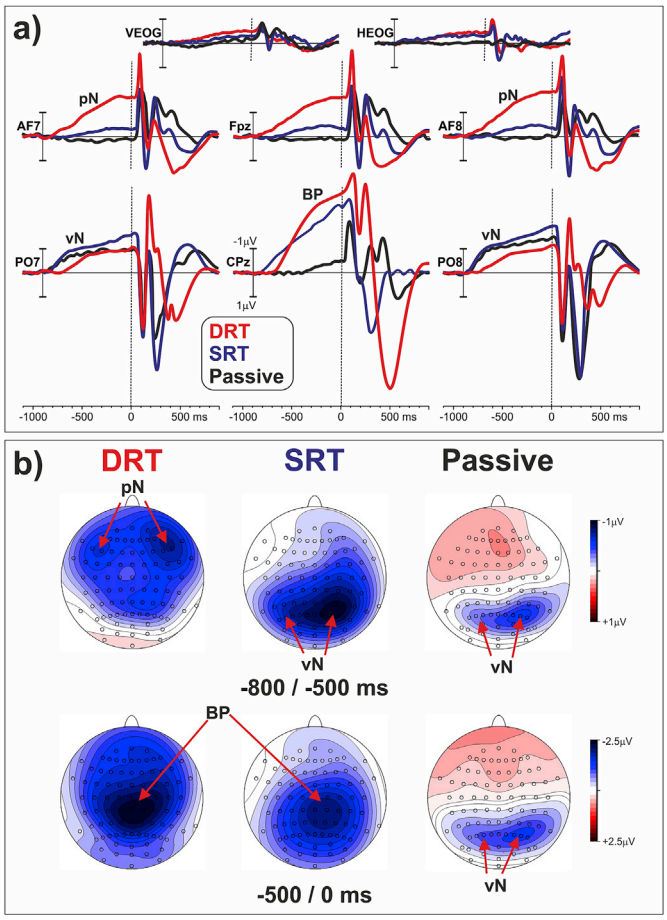

Fig. 2. Pre-stimulus. a) waveforms averaged at prefrontal, central-parietal and occipital electrodes in the three studied tasks are superimposed. b) Pre-stimulus ERP topographical voltage maps of early (−800/-600 ms) and late (−600/0 ms) time windows for the three tasks. Time zero refers to stimulus onset. The investigated ERP components i.e., the BP, the pN and the vN, are indicated.

Table 1
Mean amplitude (μV) and standards deviation of the pre-stimulus components in the interval from −800 to 0 ms. The pN is calculated pooling AF7, Fp1, Fpz, Fp2 and AF8. The BP pooling Cz and CPz. The vN pooling PO7, P7, PO8 and P8.

	pN	BP	vN
DRT	−1.19 ± .13	−1.67 ± .16	−0.98 ± .10
SRT	−0.22 ± .03	−1.23 ± .13	−1.32 ± .15
Passive	+0.05 ± .02	−0.14 ± .02	−1.03 ± .11

The ANOVA on the pN showed a significant effect of Condition ($F_{(2,70)} = 312.5$, $p < 0.0001$, $_p\eta^2 = 0.89$). Post-hoc comparisons showed that the DRT had a larger amplitude than the other two conditions ($p < 0.0001$), and the SRT had a larger amplitude than Passive ($p = 0.0007$). The effect of ROI ($F_{(1,35)} = 1.24$, $p = 0.27$) and the interaction ($F_{(2,70)} = 2.28$, $p = 0.11$) were not significant.

The ANOVA on the BP showed a significant effect of Condition ($F_{(2,70)} = 857.2$, $p < 0.0001$, $_p\eta^2 = 0.90$). Post-hoc comparisons showed

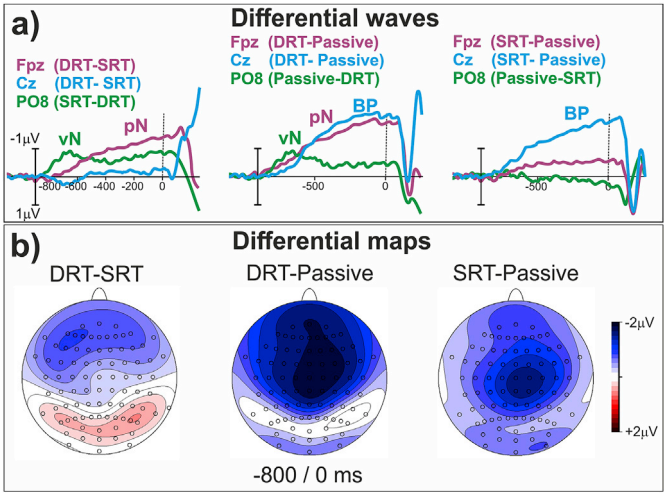

Fig. 3. Pre-stimulus differential activity. a) Pre-stimulus differential ERP waveforms comparing the three tasks at respectively relevant electrodes, which were superimposed (the differential BP, pN and vN are indicated). Note that for the PO8 channel the subtraction is inverted to obtain negative waves as for the other displayed channels. b) Topographical distribution of the differential activity showed in Fig. 3a over the entire pre-stimulus interval from −800 ms to stimulus onset. c) Statistical maps representing the scalp distribution of the significant differences between tasks, also marked by thick circles.

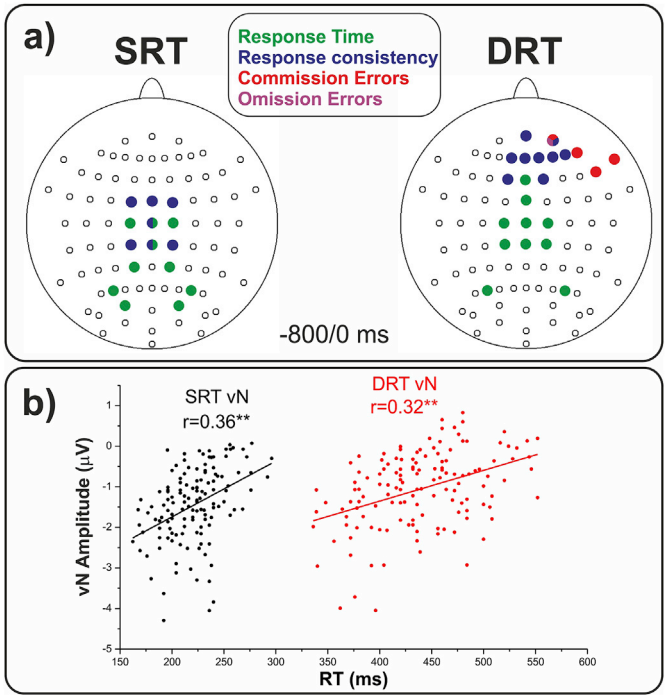

Fig. 4. Correlations. a) The coloured circles over the corresponding electrode indicate significant correlations between pre-stimulus ERP (averaged over the −800/0 interval) and behavioural performances in both DRT and SRT. b) Individual data from the correlations between the vN and the response time (RT) for both the SRT and DRT.

that the DRT had a larger amplitude than the other two conditions ($p = 0.0009$), and the SRT had a larger amplitude than Passive ($p < 0.0001$).

The vN amplitude was submitted to a 3 × 2 ANOVA with 3 Conditions (DRT, SRT and Passive) and 2 ROIs over the left and the right parieto-occipital scalp. The left ROI pooled PO7 and P5 electrodes whereas the right ROI pooled PO8 and P6 electrodes. Results showed a significant effect of Condition ($F_{(2,70)} = 258.5$, $p < 0.0001$, $_p\eta^2 = 0.82$). Post-hoc comparisons showed that the SRT had larger amplitude the other two conditions ($p < 0.0008$), which did not differ each other. The effect of ROI ($F_{(1,35)}<1$) and the interaction ($F_{(2,70)}<1$) were not significant.

Fig. 4a shows correlational analysis results between pre-stimulus ERPs and behavioral performance in the SRT and the DRT. The figure is a schematic representation that combines all the correlational data in a single image. The analysis was made on the same pre-stimulus time interval used for statistic comparisons (mean voltage from −800 to 0 ms). Thick circles represent electrodes' activities which significantly correlated with behavioral performance. For the SRT, medial central-parietal, bilateral parietal-occipital and occipital electrodes activities correlated with response time ($r > 0.39$, $p = 0.0027$): the more negative the amplitude, the lower the RT. Activity at medial frontal-central electrodes correlated with response consistency ($r > 0.30$, $p = 0.022$): the more negative the amplitude, the lower the ICV. For the DRT, medial frontal, central, central-parietal and bilateral parietal-occipital electrodes correlated with response time ($r > 0.44$, $p = 0.0012$): the more negative amplitude, the lower the RT. Medial and right prefrontal electrode activities correlated with response consistency ($r > 0.29$, $p = 0.044$): the more negative amplitude, the lower the ICV. Right prefrontal electrodes activity correlated with commission errors ($r > 0.25$, $p = 0.0165$): the more negative the amplitude, the lower the CE percentage. Only Fp2 correlated with omission errors ($r = 0.31$, $p = 0.011$): the more negative the amplitude, the lower the OE percentage. Fig. 4b shows individual data for the correlational between the vN (PO7-PO8 pool) and the RT in both the SRT ($r = 0.36$, $p = 0.0018$) and the DRT ($r = 0.32$, $p = 0.002$).

3.3. Post-stimulus ERP

Fig. 5 shows post-stimulus ERP waveforms averaged in the four conditions considered (DRT target and DRT non-target trials are shown separately). Fig. 6 shows the topography of the post-stimulus ERPs at relevant intervals. Table 2 shows the mean amplitude of the studied components. The earliest component was the C1, clearly visible in Passive task only, starting at 65 ms and peaking at 100 ms on medial central-parietal sites. The C1 was not detectable in the other conditions, probably because those required a motor response (see the discussion section). The P1, present in all conditions, initiated at 75 ms and peaked over bilateral occipital-parietal areas at 110–120 ms. The N1 (more evident in DRT, both target and non-target) peaked at 180 ms over bilateral occipital-parietal areas. The P2, visible in SRT and Passive task, peaked at 260 ms over medial and bilateral occipital-parietal areas.

The pN1, present in all conditions, initiated at 60 ms and peaked over medial prefrontal areas at 115 ms in SRT and DRT, whereas in the Passive task peaked later (130 ms) with larger amplitude. The pP1, present in SRT and DRT, peaked over bilateral prefrontal scalp at 180 ms. In the Passive task, the pP1 barely reached positive values; however, it showed a similar shape (even though delayed), as in SRT and DRT. The pP2, present in DRT only, were maximal over bilateral prefrontal scalp between 200 and 400 ms with larger amplitudes for target than non-target trials.

The N2, present in DRT only, peaked over medial frontal scalp at 290 ms. Finally, the P3 was present in SRT and DRT and peaked over medial parietal-occipital areas at 300 ms and 510 ms, respectively.

In addition to these known components, three additional novel prefrontal components could be detected. The first two have been labelled in the figure prefrontal N2 (pN2) and N3 (pN3), because their topographies are similar to the pN1. The pN2 peaked at 280 ms and the pN3 at 430 ms: they were clearly visible in the Passive task only, likely because masked by concomitant positivities (pP2 and P3) in the other tasks. Lastly, in DRT (both target and non-target trials), a prefrontal component peaking at 465 ms was also detectable and labelled prefrontal P3 (pP3).

Fig. 7 shows (by subtraction) the comparison among post-stimulus ERP obtained in the three tasks in terms of temporal evolution (Fig. 7a) and spatial topography (Fig. 7b); only differential activities were

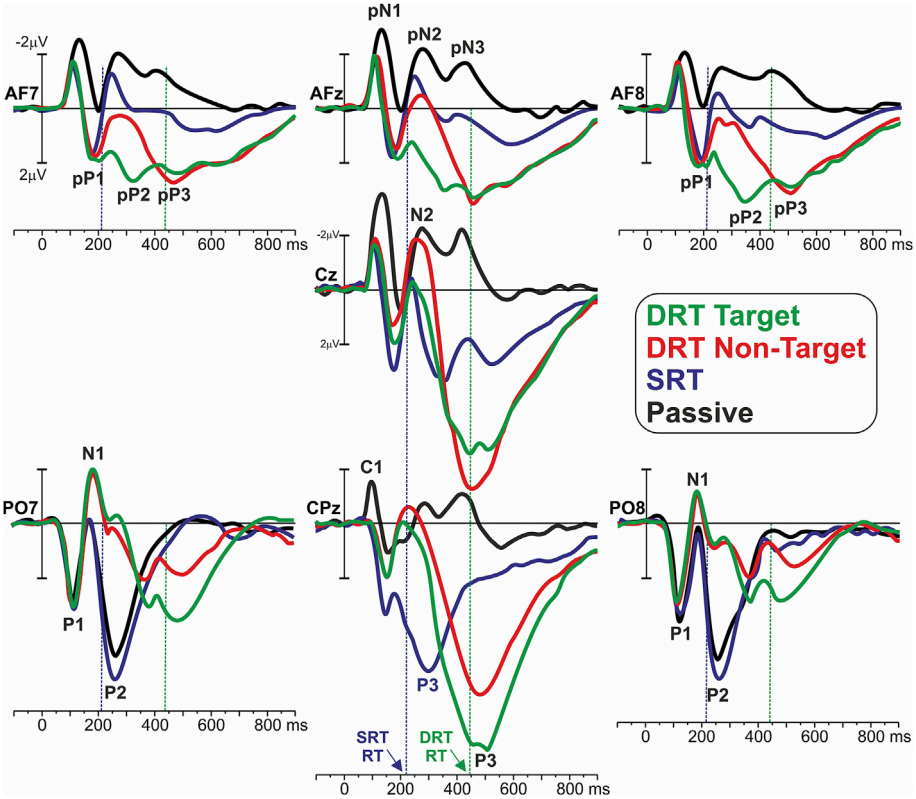

Fig. 5. Post-stimulus. Waveforms at prefrontal, central, centro-parietal and occipital electrodes. The waveforms obtained in the three tasks and four conditions (DRT target and DRT non-target trials are shown separately) are superimposed to facilitate comparison. The considered ERP components are labelled, and response time (RT) are indicated by dotted lines and arrows.

considered in this figure. Comparing SRT and Passive task, the pP1 was larger in SRT; by subtraction, emerged the pN2 and pN3, which were mainly detectable in Passive task, and the P3 that was visible in SRT only. Comparing DRT target with Passive task, amplitude differences on the pP1, pP2 and P3 were large and peaked at 150, 270 and 450 ms. Comparing DRT non-target with Passive, amplitude differences on the pP1, Pp2 and P3 were present at the same peak latencies measured for DRT target, except for the non-target P3 that peaked earlier (at 435 ms). Finally, comparing DRT target with DRT non-target, strong effects were detected only on the differential pP2 (dpP2) peaking at 300 ms, and on the differential P3 (dP3) peaking at 490 ms. The dP3 was present not only around the P3 peak (CPz) but also on left frontal areas, producing the typical tangential distribution of activity in sensorimotor areas contralateral to the responding hand.

ANOVA on the P1 showed no significant effects, being comparable among conditions and ROIs. The N1 showed a significant effect of Conditions ($F_{(1,105)} = 257.9$, $p < 0.0001$, ${}_p\eta^2 = 0.92$). Post-hoc comparisons showed that the N1 for both DRT conditions (target and non-target, which did not differ each other) were larger than the SRT and Passive ($p < 0.0001$), which did not differ. ANOVA on the pN1 showed the effect of Conditions ($F_{(3,105)} = 123.3$, $p < 0.0001$, ${}_p\eta^2 = 0.87$). Post-hoc comparisons showed that the pN1 in the Passive condition was larger than the other conditions ($p < 0.0001$), which did not differ each other. ANOVA on the pP1 showed a significant effect of Conditions ($F_{(1,105)} = 145.1$, $p < 0.0001$, ${}_p\eta^2 = 0.89$). Post-hoc comparisons showed that the pP1 in the Passive condition was smaller than the other conditions ($p < 0.0001$), which did not differ. ANOVA on the pP2 showed a significant effect of Conditions ($F_{(1,35)} = 167.4$, $p < 0.0001$, ${}_p\eta^2 = 0.95$), of ROIs ($F_{(1,35)} = 85.3$, $p < 0.0001$, ${}_p\eta^2 = 0.95$), and interaction ($F_{(1,35)} = 612.5$, $p < 0.0001$, ${}_p\eta^2 = 0.97$). Post-hoc comparisons on the interactions showed that the pP2 was larger for target than non-target ($p < 0.0001$) and was larger at AF8 than AF7 for target ($p = 0.0005$). ANOVA on the N2 showed a significant effect of Conditions ($F_{(1,35)} = 32.3$, $p < 0.0001$, ${}_p\eta^2 = 0.86$). Post-hoc comparisons showed that the N2 was larger for non-target than target condition ($p = 0.0002$). No effects of ROIs and interactions were found. ANOVA on the P3 showed a significant effect of Conditions ($F_{(1,35)} = 49.7$, $p < 0.0001$, ${}_p\eta^2 = 0.86$). Post-hoc comparisons showed that the P3 was larger for target than non-target condition ($p < 0.0001$). No effects of ROIs and interactions were found.

Correlational analyses between ERP peak latency and response time in SRT and DRT are reported in Fig. 8a. Results indicate highly significant positive correlation between the dpP2 and RTs ($r = 0.69$ $p < 0.0001$), and between the P3 and RTs in both tasks (SRT $r = 0.57$ $p < 0.0001$, DRT $r = 0.50$ $p < 0.0001$). The dashed 45° oblique line represents the equivalent time of electrophysiological component peak and behavioral RTs. The figure shows that while the P3 peak follows the motor response, the dpP2 (and therefore the target pP2) precedes the motor response by 100–150 ms. Fig. 8b shows significant negative correlations between RTs and error rates expressed as a percentage of CE ($r = 0.54$, $p < 0.0001$), and OE ($r = 0.38$, $p < 0.0002$). In other words, the faster the response, the higher the error rate, in line with speed-accuracy trade-off (Bogacz et al., 2010).

3.4. Source analysis

Source localization was first used to gather more information on the anticipatory visual component vN described here for the first time. To this aim, we used the ERP recorded in Passive vision, because in this condition the pN and the BP were not present.

Since the topography of vN component is bilateral, (as first step using BESA analysis) a symmetric dipole pair was fitted between −800 ms and stimulus onset; the pair resulted localized in bilateral extrastriate visual areas. As a second step a single source was fitted in the C1 time window (80–100 ms). After that, the pN1 was fitted in the 100–140 ms interval

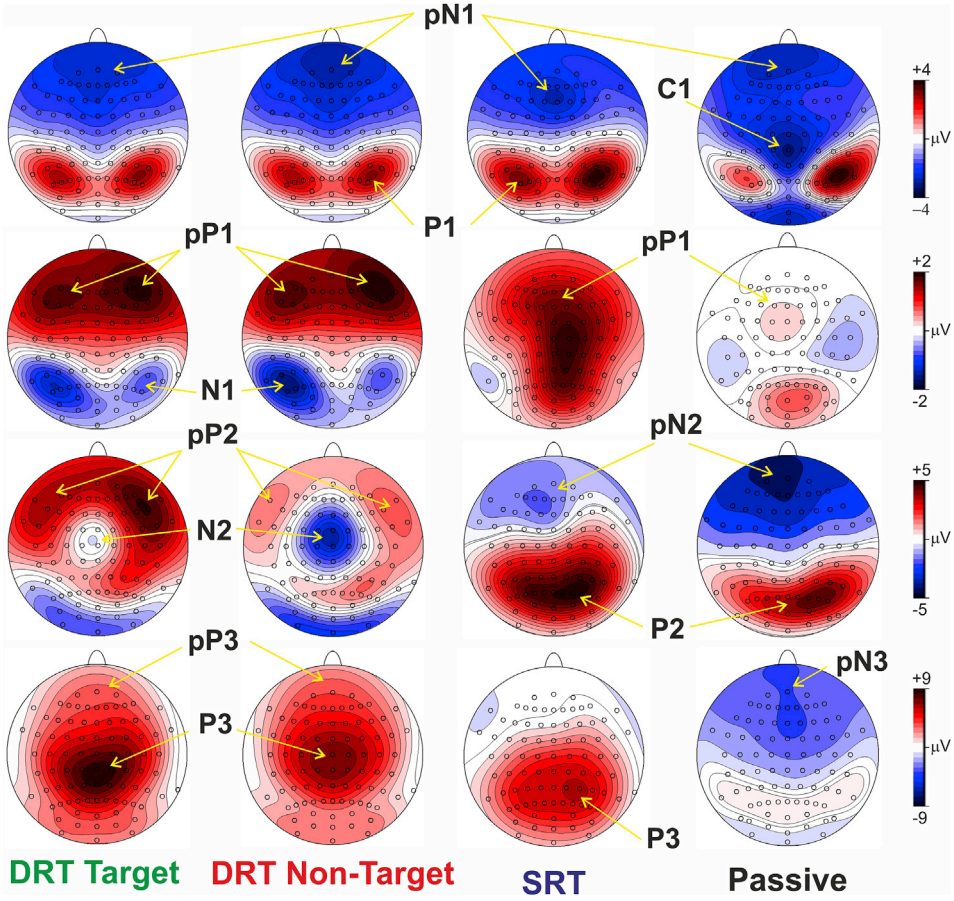

Fig. 6. Post-stimulus maps. Topographical distributions of components are shown separately for the three tasks.

Table 2
Mean amplitude (µV) and standard deviations of the post-stimulus components. The C1 was measured at the CPz-Pz pool. The P1, the N1 and the P2 at the PO7-PO8 pool. The pN1, the pN2 and the pN2 at the Fpz-AFz pool. The pP1, the pP2 and the pP3 at the AF7-AF8 pool. The N2 at the Fz-FCz-Cz pool. The P3 at the Cz-CPz pool. *NP* = not present.

	C1	P1	N1	P2	pN1	pP1
DRT Target	*NP*	3.22 ± .42	−1.95 ± .24	.23 ± .05	−1.98 ± .21	1.93 ± .19
DRT Non-Target	*NP*	3.19 ± .40	−1.93 ± .20	.31 ± .04	−1.96 ± .20	1.88 ± .22
SRT	*NP*	3.15 ± .36	-.17 ± .02	5.74 ± .65	−1.97 ± .23	1.53 ± .17
Passive	−1.48 ± .16	3.09 ± .32	-.12 ± .02	4.85 ± .53	−2.88 ± .30	0.16 ± .03
	pP2	**N2**	**P3**	**pN2**	**pN3**	**pP3**
DRT Target	2.74 ± .32	-.31 ± .34	7.97 ± .81	*NP*	*NP*	2.77 ± .31
DRT Non-Target	.59 ± .61	−1.77 ± .21	5.97 ± .66	-.49 ± .05	*NP*	3.15 ± .37
SRT	.09 ± .01	-.42 ± .05	5.12 ± .58	−1.06 ± .17	*NP*	0.58 ± .07
Passive	−1.52 ± .18	−2.19 ± .26	*NP*	−2.08 ± .21	−1.51 ± .17	*NP*

with a dipole pair. BESA fitting localized the C1 in medial occipital cortex (striate area) and the pN1 near the anterior insular cortex. This four-dipole model explained 94.5% of ERP variance in the −800/140 ms interval of the grand-averaged ERPs (mean residual variance, RV, 5.5 ± 0.4%). Fig. 9a shows the source model with the dipole localization rendered on an anatomical template (sagittal view), and the sources time-course over the whole referred period. These waveforms show that extra-striate areas were likely the origin of the vN, the P1 and, at least partially, the P2. To verify that this pre-stimulus extrastriate activity (the vN) was genuine and not due to noise, the dipole time-course (dipole moment) from −900 to 0 ms was submitted to *t*-test against zero that showed a significant difference from −730 to 0 ms ($p < 0.01$). Activity originating in the striate visual area (V1) well explained the C1 and the subsequent reactivation called C2 and C3, as described elsewhere (Di Russo et al., 2005, 2012; Odom et al., 2004; Pitzalis et al., 2018). The anterior Insula activity explained the pN1 and the pP1. Moreover, activity originating in this area explained the pN2 and the pN3. Fig. 9b shows the 3D ERP topography (current source density, CSD, maps) indicating similar scalp distributions of the vN and the P1 components, although with opposite polarity. Fig. 9c shows the 3D CSD topographies of activities generated in the time interval between 100 and 140 ms after stimulus by the two sources of Fig. 9a localized in the anterior insula and extra-striate areas, respectively. The map indicates a clear spatial separation of the two cortical generators.

An additional evaluation of the vN component was performed using the distributed-source approach of the eLORETA. Fig. 10a shows the results of *t*-test against zero in the −800/0 ms interval which shows significant activation in the bilateral occipital cortex (mainly in correspondence of the transverse occipital sulcus, in between areas MT and V3A, and slightly extending ventrally toward the collateral sulcus and

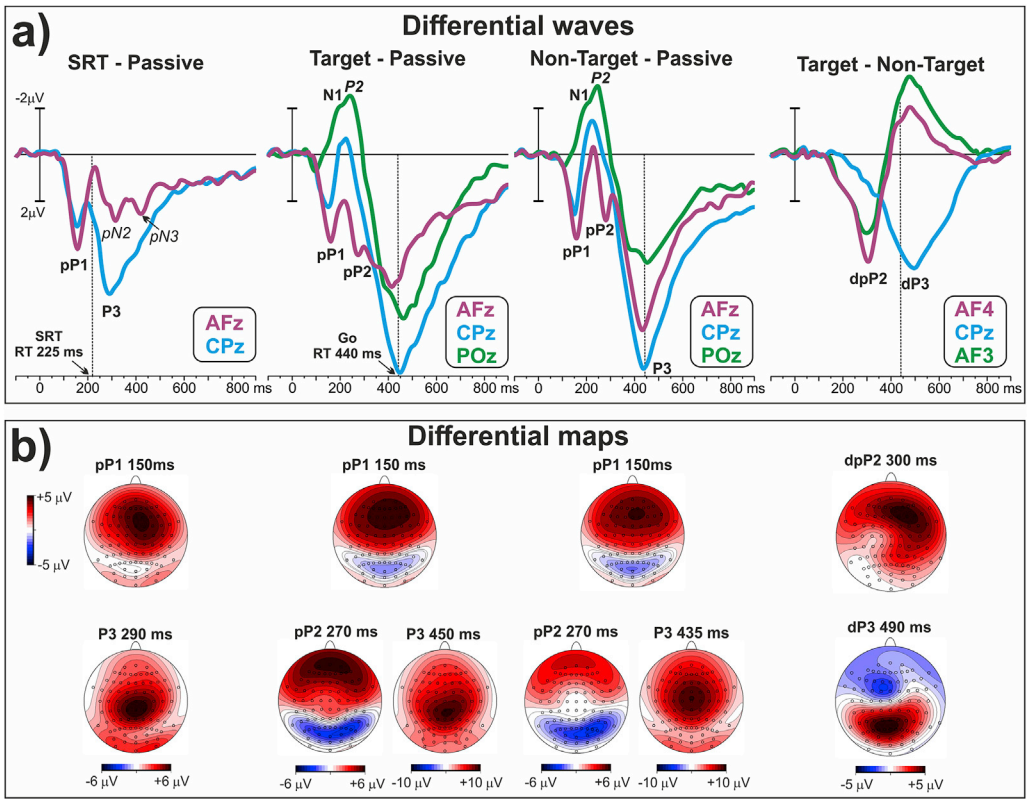

Fig. 7. Post-stimulus a) Differential ERP waveforms comparing the three tasks and four conditions (DRT target and DRT non-target were considered separately) at the relevant electrodes. Subtractions at different electrodes were superimposed and reported with distinct colors. b) Topographical distribution of the differential activity displayed in panel a. c) Statistical maps representing the scalp distribution of the significant difference between tasks.

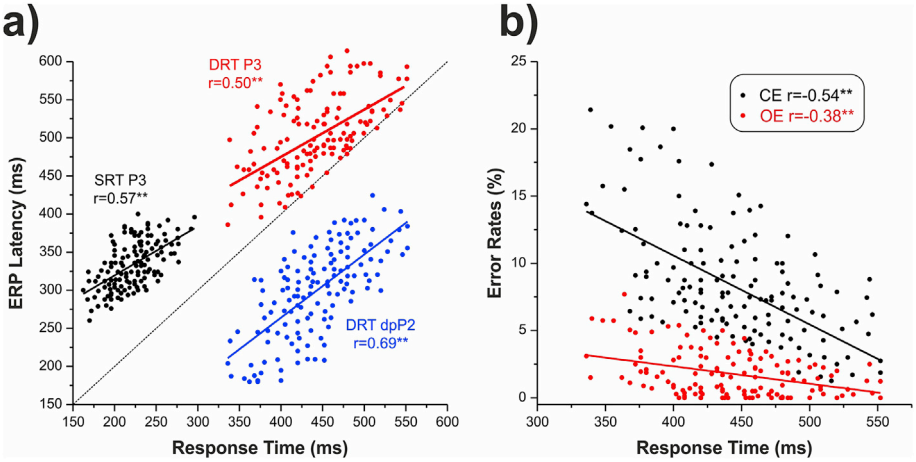

Fig. 8. Post-stimulus differential activity a) Correlations between latency of ERP components P3 and differential Pp2 (dPp2) and response time. The diagonal line represents the equi-latency point. b) Correlation between error rates (CE and Om) and response time.

fusiform gyrus), confirming the hypothesis of the extrastriate source for the vN component. Fig. 10b shows the result of *t*-test against zero at the P1 peak (110 ms) indicating similar foci of activity with the vN component, with the only difference residing in the presence of the foveal representations of early visual areas V1 and V2 in this early stimulus processing stage.

Additional source analyses were also performed for all studied conditions. Fig. 11 shows time-courses of source models for all conditions (mean RV, 6.2 ± 0.6%). Source locations in these complex models were seeded (fixed in place) according to previous fMRI data (Di Russo et al., 2016; Sulpizio et al., 2017); present analyses support the described ERP results. Taken together with previously published data, present results highlight the contribution of extra-striate areas during the preparation phase in both passive vision and SRT; this contribution is small in DRT, which is dominated by a strong iFg influence. Furthermore, these models show the preparatory activity in the anterior intraparietal sulcus (aIPs) of the left hemisphere contralateral to the used hand. In all conditions, t-tests against zero were run in the −900/0 ms interval, and significant differences were found for the iFg sources in the DRT (−610/0 ms, $p < 0.001$) and in the SRT (−400/0 ms, $p < 0.003$). For the SMA-CMA sources, significant differences were found for the DRT (−452/0 ms, $p < 0.001$), the SRT (−720/0 ms, $p < 0.001$), and, to a lesser extent, for the passive condition (−380/0 ms, $p < 0.002$). The left aIPs source was different from zero in both the DRT and SRT in the −540/0 ms interval ($p < 0.005$).

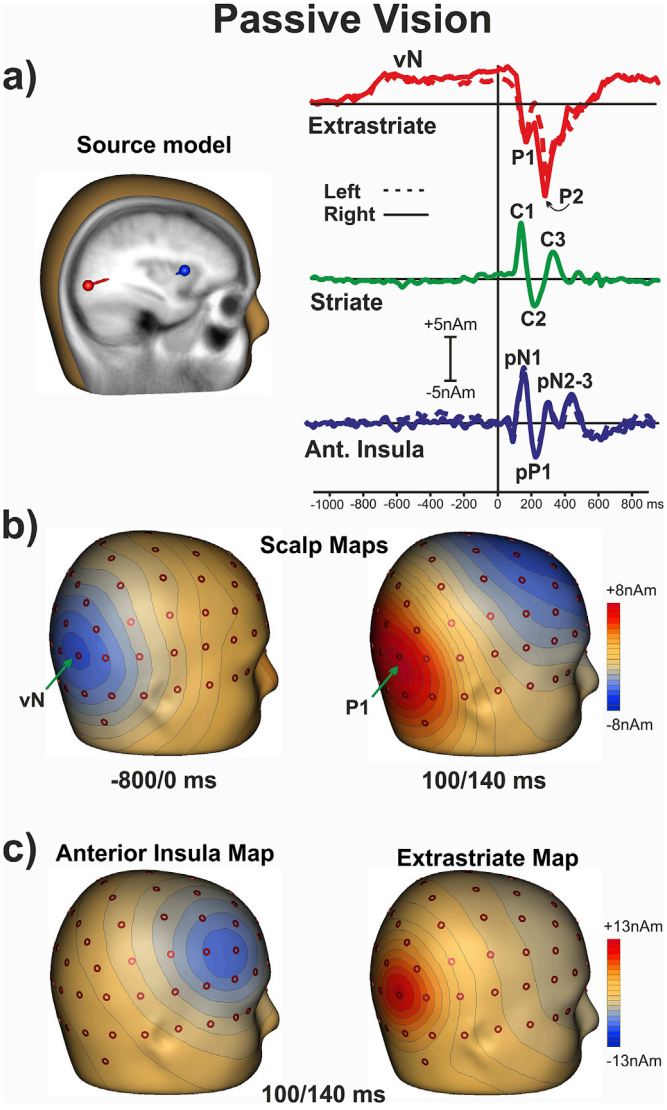

Fig. 9. BESA source localization of passive vision ERP over both pre- and post-stimulus periods. a) The fMRI head template indicates the locations and orientations of the extrastriate and insular sources. The waveforms indicate the time-course of the modelled brain sources. b) Realistic topographical scalp topography of the sources in the anterior Insula and in the extrastriate areas.

In the post-stimulus phase, various results are noteworthy. First, the insular cortex might be the origin of the pN2 and pN3 components. Second, the DRT N2 is mainly explained by the negative peak of frontal CMA and SMA activity. Third, data show that multiple cortical generators contribute to the P3 that originated mainly from the posterior Intra-parietal sulcus (pIPs), the SMA-CMA, the aIPs and M1-S1, however, the aIPS and the S1-M1 were present only for DRT target and SRT conditions. Fourth, the DRT non-target model gives some hints on the presence of another novel prefrontal component found in the present study, the pP3, which is concomitant to the P3, but localized bilaterally in the iFg. All the insular components were different from zero at their peaks ($p < 0.0012$), except for the pP2 in the non-target DRT. Other non-significant activities were found for the left M1-S1 sources in the non-target DRT and passive conditions, and in all conditions for the right M1-S1 and the aIPs.

4. Discussion

In the present work, we selected a large sample of high-quality EEG data with the initial aim of providing an accurate description of

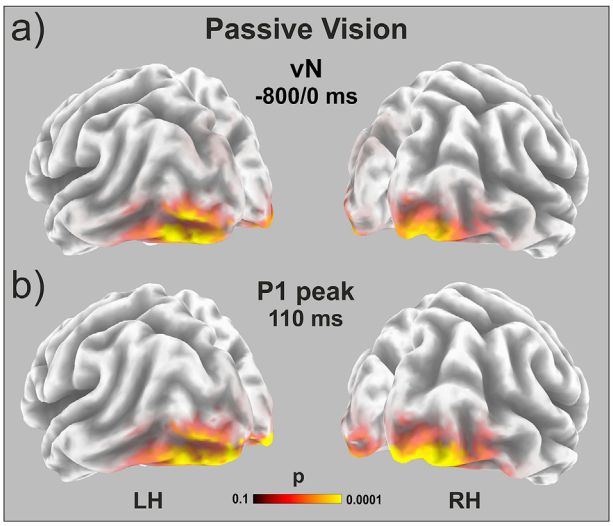

Fig. 10. e-LORETA source localization of passive vision. a) Brain areas significantly active during the −800/0 ms pre-stimulus phase (the vN) in the passive vision task. b) Same analyses made at the P1 component peak at 110 ms.

distinctive pre- and post-stimulus ERP components observed during three tasks: Passive viewing, SRT and DRT. For both pre- and post-stimulus phases, we coupled scalp-recorded waves with their neural sources (based on present source analysis and fMRI results from previous studies), and behavioral data. We showed that distinctive scalp-recorded brain activities characterize the tasks during both task preparation and stimulus processing. In the preparation phase, we described readiness activities within frontal, prefrontal and occipital areas. In view of the large sample of selected participants, present data can be considered as normative for the adult population in the 18–45 years age range for the three considered tasks.

4.1. Pre-stimulus phase

4.1.1. Occipital activity: the vN component

In the case of the passive task, we found that waiting for visual stimuli activated the extra-striate areas. This ERP component has not been previously described (just briefly mentioned for the passive and SRT conditions by Perri et al., 2018b); we propose to name it visual negativity (vN). The vN might represent the scalp-recorded correlate of the visual readiness activity, emerging bilaterally over extrastriate occipital sites. Further, the vN component was also detected in the SRT condition, where participants had an active task and waited for the stimulus to respond as soon as possible with their hand. Indeed, differential waves at PO7 suggest that the level of activation was comparable in Passive and SRT. In DRT, the vN amplitude was smaller, likely because masked by concomitant activity, especially the very large BP. Further, one may propose that in the DRT, the necessity of stimulus categorization as target or non-target, which could take place only after stimulus presentation and evidence accumulation, may limit visual readiness with respect to SRT. The differential waves at occipital level (Fig. 3a), suggesting a delay in the activation of occipital regions in DRT with respect to both SRT and Passive task, supports this interpretation.

Particularly interesting are the correlations between preparatory brain activities and behavioral performance, i.e. RTs and accuracy, as summarized in Fig. 4. For the SRT, RTs positively correlated with both vN and BP amplitudes (the greater the amplitude the shorter the RT). While a direct relationship between motor preparation and time of motor response (BP-RT correlation) has been already reported (Perri et al., 2014b, 2015), the correlation between the vN component and the RTs is a novel result of the present study, which supports the view that extra-striate activation before stimulus reflects its involvement in a

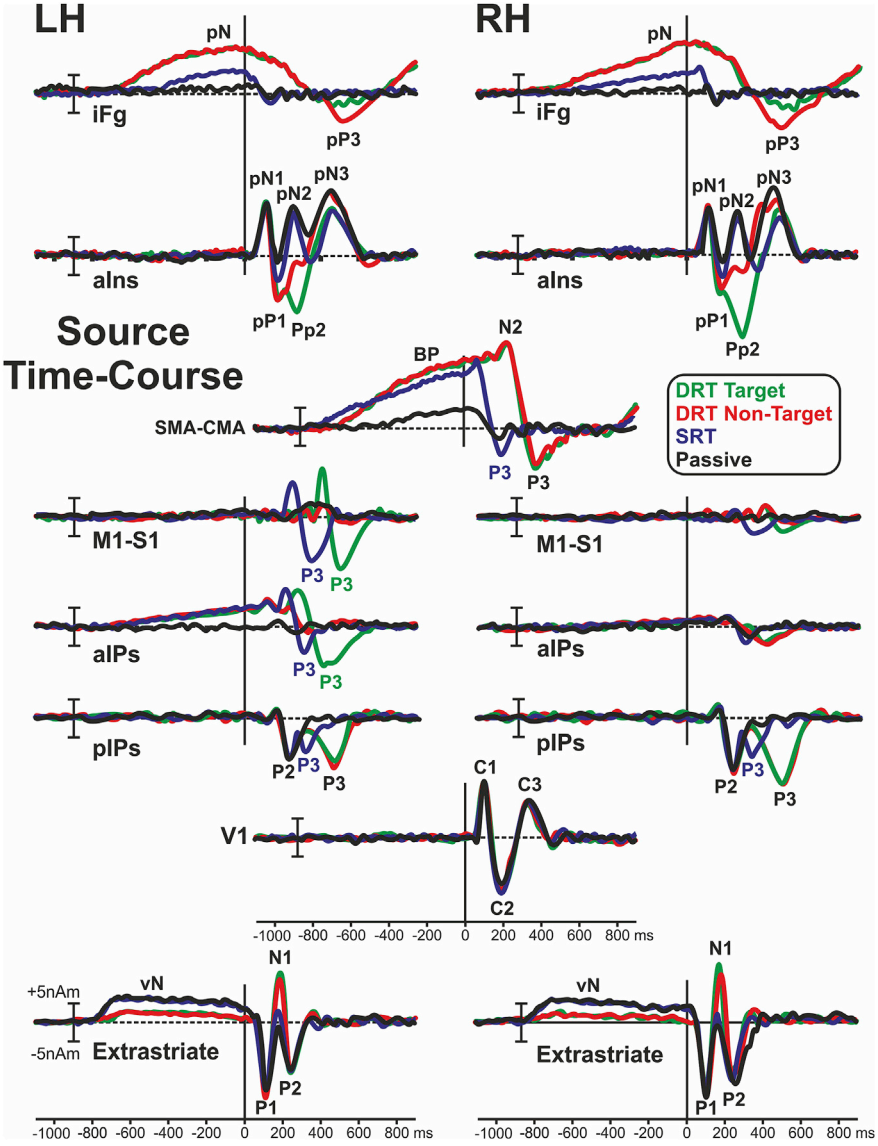

Fig. 11. BESA Source models for all tasks expressed as the time-course of the modelled brain sources.

preparatory neural network, possibly contributing to increasing the stimulus-processing speed, and likely representing a sort of "visual readiness" similar to the "motor readiness" (Kornhuber and Deecke, 1965).

The vN may reflect perceptual enhancement of the incoming stimuli as a general result of attention (Thut et al., 2006; Busch and VanRullen, 2010). Although the vN has never been directly reported, it is conceivable that occipital activity reported in some CNV studies (Brunia et al., 2011), particularly those involving selective attention (Gómez et al., 2003; Gómez et al., 2007), might share common patterns with the vN reported in the present study. Also, the anticipatory SPN, usually interpreted as an expectation index of upcoming visual feedbacks on previous performance (van Boxtel and Böcker, 2004), may contain vN-like activity. However, the vN and the SPN topographies differ, because the SPN peaks at prefrontal and parietal sites, whereas the vN shows occipital activation. Finally, the vN is present in the Passive task, while the SPN and the occipital activity reported in CNV studies were reported in complex motor tasks.

Admittedly, in previous studies using the same SRT and DRT, we did not focus on the vN activity. The vN was not prominent as the BP or the pN in Di Russo et al. (2016) and consequently we did not report and discuss the occipital activity. However, small negativities at parietal-occipital site are detectable in the last 400 ms before the stimulus onset reaching about 1 μV at stimulus onset (see Fig. 2a; PO8 electrode in that study), an amplitude value that is not far from the present value. The vN reduction (particularly the delayed onset) in that study could be due to the presence of cues (absent in the present study), the very long ISI (5250–6750 ms) used to allow fMRI scanning, and also the relatively limited number of subjects (21) with respect to the present sample.

About the vN nature, in order to exclude that a persistent occipital activation due to the visual stimulus of the previous trial could be responsible for the vN, we re-averaged present data comparing short (<1400 ms) with long (>1600 ms) ISIs. Results (Supplementary Fig. 3) showed that the vN did not differ between these sub-averages in any task (passive, SRT and DRT). Moreover, we replotted (see Supplementary Fig. 1) the ERP data from Quinzi et al. (2018) using an identical DRT as in the present study, but with a longer and more variable ISI (2000–4000), and a limited number of subjects (N = 14). The clear vN presence with such a long ISI may exclude any effect from the previous stimulus.

To the best of our knowledge, the vN is the first ERP clear evidence of "visual anticipation" postulated by Bayesian models of the predictive brain (e.g. Knill and Richards, 1996; Mamassian et al., 2002). These models proposed the combination of top-down generative components (here possibly represented by the vN) with bottom-up processing;

low-level cues distribution of activities (the vN) would activate high-level models (the P1). This top-down process may facilitate responses speed in simple tasks requiring low cognitive involvement as in SRTs.

4.2. SMA-CMA (the BP component), prefrontal (the pN component) and aIPs activities

Confirming previous studies with SRT and DRT, we found an intense motor preparation at SMA and CMA level reflecting the well-known BP component. Moreover, in DRT, the iFg was strongly and bilaterally activated (the pN component) while the subjects expected the stimulus for decision-making about acting or not acting. The pN was interpreted as an inhibitory control activity concomitant to the growing motor preparation in SMA and CMA; for comparable results and interpretation, see Di Russo et al. (2016). In the present study, a small activity in the right iFg (the pN) was found also in SRT. This latter component was negligible in previous SRT studies possibly because the number of participants was smaller and included participants of younger mean age; indeed, the pN become evident in old adults (Berchicci et al., 2012).

It is interesting to evaluate the correlation between ERPs and behavioral data. As described above, the BP-RT correlations have been frequently reported (Bianco et al., 2016; Bianco et al., 2017a; Perri et al., 2014b, 2015) and were confirmed in the present study. With such a large sample, we could also focus on the accuracy in the task (the number of errors is low at the individual level) and its relationship with the pN component. Commission errors in DRT negatively correlated with right prefrontal activity (pN), indicating that the smaller the amplitude of the pN component, the higher the number of false alarms. This result may support a functional interpretation of the right pN in terms of inhibitory control; in the case of decreased control, the subject was less able to prevent undesired responses (e.g. Aron et al., 2004). Moreover, omission errors negatively correlated with the pN amplitude in DRT, although the effect was present at Fp2 only (the smaller the amplitude, the higher the number of omissions). These findings may support a general interpretation of the pN in terms of proactive cognitive control, including attentional inhibitory control and prevention of a second error (Perri et al., 2016, 2017): when the cognitive control is low, as in the case of lapses of attention, the subject fails to respond to the target. This conclusion is also reinforced by the positive correlation between the pN amplitude and response time consistency (ICV), indicating that the higher the pN (i.e. cognitive control) the more consistent the RT values. Omission errors were almost absent in SRT; in this task, the prefrontal activity was negligible (below 0.5 μV, see Fig. 2a and b), although detectable given the large number of participants even in this simple task. Overall, results suggest that SRT involves low prefrontal control, and performance is directly regulated by preparatory activities at both motor (the BP; Berchicci et al., 2016; present study) and sensory level i.e., the vN discussed above. In conclusion, while the DRT requires a strong prefrontal control over motor preparation, the SRT is mostly regulated at motor and perceptual levels. Overall, our previous proposal of interpreting the BP-pN components as a sort of proactive acceleration-brake system (Di Russo et al., 2016; Bianco et al., 2017b) is corroborated by correlations with the behavioral data, and the vN findings further completed the picture introducing a proactive sensory anticipation facilitating the upcoming stimulus detection.

In both SRT and DRT, the source analysis time-course (Fig. 11) showed a small slow-growing parietal activity localized in the left aIPs, concomitant to the large SMA-CMA activity. This aIPs activity may be associated with the parietal involvement reported in some CNV studies (Van Boxtel and Boker, 2004; Gómez et al., 2003; 2007), although the difference between tasks does not allow a valid comparison. Alternatively, this parietal preparatory activity could be related to the "posterior BP" found in self-paced grasping tasks (Bozzacchi et al., 2012), and, therefore, associated to sensory-motor spatial integration function of this area (Filimon, 2010). Notably, a small growing activity at the SMA-CMA level was present also in Passive task, while no aIPs activity was detected; thus, the parietal preparation found in SRT and DRT might represent an effector-related regulating aspect, whilst the frontal BP might reflect a sort of "default" preparation to move, at least in part independent from instructions. A small preparatory activity at SMA-CMA level was also reported in a recent study during the decision stage of the task (the subject had to decide whether to press a key or not in a future time), even when the subject decided not to move (Bianco et al., 2017b). Therefore, the reported SMA-CMA activity in the present Passive task supports the view that any decision (Bianco et al., 2017b) or commitment (by instructions, present data) about future action, *including not acting* (see passive vision), may be mapped within pre-motor cortices with graded level of activation depending on the task. Future research will foster this interesting hypothesis.

4.3. Post-stimulus phase

Present findings in the Passive task confirm previous studies (for a review see Di Russo and Pitzalis, 2014), reporting activities in striate and extrastriate areas, which include triple activation in primary visual areas (V1): one feedforward (the C1) and two re-entrant feedback (the C2 and the C3) activities; these latter were rarely but consistently reported in literature (Di Russo et al., 2005, 2012; Odom et al., 2004; Pitzalis et al., 2018) and, although detectable in Passive task, are not labeled in Fig. 5. The C1 represents the first volley of visual information in V1, and, therefore, it is an obligatory and ubiquitous phenomenon in the visual domain; however, this component was not detectable in SRT and DRT. An explanation for this apparent lack of consistency could lie in the pre-stimulus baseline: at the CPz electrode (Fig. 2a) large negativity characterizes both SRT and DRT up to stimulus onset (the BP and the vN combination), but such negativity is barely detectable in passive vision. When a standard peri-stimulus baseline is applied as in Fig. 5, this negativity is set to zero and the rising shape is flattened by filtering procedures. Thus, in visuomotor tasks, the BP and the vN together likely cover the C1 component.

The extrastriate-generated P1, N1 and P2 components were present in all tasks with similar amplitude, except for the N1 that was twice larger in DRT than SRT and Passive task. The more demanding nature of DRT compared to the other tasks offers a clear explanation for this effect, since enhanced N1 amplitude reflects increased attention to the features of the stimulus to be discriminated (e.g. Luck et al., 1990).

4.3.1. The anterior insula activity

The earliest anterior Insula (aIns) activity was reflected by the pN1 component, clearly detectable in all conditions. The pN1 had early onset (60 ms) concomitant to the V1/C1 onset and peaked at about 100 ms concomitant to the peak of the posterior P1. In the passive vision, the pN1 was followed by two other negative peaks, labelled pN2 and pN3 (Fig. 5); these waves were masked in SRT and DRT by concomitant positive activities of the pP2 and the P3 components. The pN2 and pN3 components have never been described but could be detected in a recent study (Perri et al., 2018b) devoted to the study of the pN1 and the pP1 and suggesting that these components may reflect perceptual awareness and visual motor integration, respectively; the same study confirmed the insular origin of these components by independent source analysis methods. The association of the pN1 with perceptual awareness has been confirmed in a study on cortical blind patients (Sanchez-Lopez et al., 2017). The pN1, pN2 and pN3 might reflect a sequence of activation and re-activation of the aIns (similar to the activation and reactivation observed at occipital level) possibly indicating progressive stages of the perceptual awareness process.

The pP1 was present in both SRT and DRT and almost absent in Passive task; this confirms the proposal of its possible role in top-down visual-motor integration, namely the awareness of the need of motor-perceptual coupling (Perri et al., 2018a,b). Considering also that both the pN1 and the pP1 were detectable in stimulus-locked, but not in movement-locked ERPs (Berchicci et al., 2016), present data support the

view of a perceptual role of the anterior Insula (Sterzer and Kleinschmidt, 2010; Wiech et al., 2010) including perceptual awareness (Craig and Craig, 2009).

The component emerged clearly in DRT target trials, was small in DRT non-target trials and absent in the SRT and Passive; this confirms the view that the pP2 may reflect decisional processes upon action execution following stimulus discrimination (Perri et al., 2018a,2019; Perri and Di Russo, 2017; Potts et al., 1996; Ragazzoni et al., 2019) and sensory evidence accumulation (e.g. Di Russo et al., 2017). Although the P3 has been previously correlated to decisional processes (e.g. Nieuwenhuis et al., 2005), we suggest that the pP2 may be more suitable for this role. Indeed, the pP2 peaks earlier than the P3 and about 100–150 ms before the motor response; in contrast, the P3 peak generally follows the response (Fig. 8a), likely reflecting the outcome of internal decision-making processes (e.g. Nieuwenhuis et al., 2005).

Spatial and functional dissociation between the concomitant anterior (pN1 and pP1) and posterior (P1 and N1) components has been show in several studies (Perri et al., 2018a; b,2019); in the present work, we confirm the spatial separation of these insular components from posterior activity using both CSD mapping (Fig. 9c) and source analysis (Fig. 11). In addition, we extend this notion to the pN2, pN3 and pP3. Functional dissociations were also found here between the anterior and posterior components in terms of amplitude modulation among the studied conditions.

4.3.2. The iFg activity

Source analyses indicated that iFg activity was present not only in the pre-stimulus phase (as reflected by the pN component), but also in the post-stimulus phase (particularly evident in DRT; see Fig. 11). Further, the slow-raising pN returns to the baseline values immediately after the pP2 peak at 300 ms for DRT target trials. Considering that the pN was associated with attentional inhibitory control, the timing of such post-stimulus decrement suggests that for target trials, inhibition terminates when stimulus-response mapping process (the pP2) is over. Then the iFg activity remains stable at baseline level for target trials, whereas it became positive for non-target trials, as reflected by the growing pP3 component. The iFg activity increment during the pre-stimulus phase (pN), its post-stimulus decrement and polarity change (pP3) in non-target trials (likely explained as persistent inhibition) is consistent with the view that iFg activity could reflect a sort of top-down control on task execution (Perri and Di Russo, 2017), and confirms the close relationship between the aIns and the iFg in exogenous attention, particularly when visual stimuli are coupled to motor response (Corbetta et al., 2008).

4.3.3. Correlation between post-stimulus ERPs and behavior

Consistent with previous literature (e.g. Ouyang et al., 2017), the P3 latency correlated with RTs for both SRT and target DRT; however, as noted above, the P3 peak generally follows or is concomitant to the motor response, a feature consistent with the idea that the P3 peak may reflect cognitive processes associated with the outcome of decision, such as memory updating (e.g. Polich, 2007), post-decision closure mechanism (e.g. Desmedt, 1980) and/or response selection (Verleger et al., 2014) confirming the P3 multifunctional origin. Taking into account also source analyses (Fig. 11), present data confirm previous ERP-fMRI studies (Di Russo et al., 2016; Ragazzoni et al., 2019; Sulpizio et al., 2017), showing that in the present tasks the P3 is a complex wave resulting from activity of many cortical areas associated with motor response preparation and execution, including SMA, CMA, aIPs, pIPs, iFg, M1 and S1. Depending on the task, other brain areas were associated with the P3 (for a review see Linden, 2005). In conclusion, the correlation between P3 latency and RTs may reflect the correlation between multiple cortical processes taking place in a wide timeframe. In contrast, it is interesting to note that the high correlation ($r = 0.69$) between RTs and the pP2 peak latency indicates that this novel prefrontal component *predicts* the RTs about 100–150 ms before the motor response (Fig. 8a). This novel result confirms the aIns role in response-related evidence accumulation and stimulus-response mapping (Perri et al., 2017).

5. Limitations and future research

The present large sample ERP data can be considered normative data, but limitations must be acknowledged. First, data refer to Caucasian adults from 18 to 45 years, with medium-high socioeconomic status and education level, and physical fitness level ranging from moderate to high (2–10 h of exercise per week). It would be interesting to collect additional data in elderly participants since the few data on elderly show that prefrontal components are modulated by age (Berchicci et al., 2013). Further, the fitness of participants seems to play a role among elderly subjects. Pursuing the abovementioned goals require additional recruitment. Further, the present study does not separate males and females' data; ERPs literature on gender difference shows contrasting results which, at least in part, may be explained by the limited sample of the studied groups. The availability of larger datasets would allow this analysis. However, considering the relevance of the gender differences topic and the wide literature involved, we will analyze and discuss gender differences in a dedicated paper. Second, there are general limitations regarding the used source analysis methods, particularly when combined with fMRI measures, such as the lack of physiological equivalence between BOLD signals and ERP activity (see Puce and Hämäläinen, 2017 for a review) or the impact of posture on brain activity (see for instance, the shift in the low frequency brain activity in supine and vertical position; Spironelli et al., 2016). These problems are minimized in the present study because the fMRI coordinates were not used for all the source analyses (Figs. 9 and 10), and when introduced (Fig. 11), were used only as a starting model in which the source activity was calculated on ERP data. The large sample used should minimize inter-individual differences in electrodes' placement and other drawbacks in using source analyses, pointing at an “average brain” as a stand-in for any individual's anatomy. Indeed, the variations in individual brain anatomy should be counterbalanced by the use of a large number of participants. Third, the trial averaging procedure, commonly used in ERP analysis, does not allow to detect possible inter-trial variability, which may play a role in cortical function (Arieli et al., 1996). A future study on the present dataset using single-trial approaches could investigate cortical preparation associated with a given RT (or a small RT range) averaged across participants (Delorme et al., 2015). Fourth, present study considers only visual and visuomotor tasks; future studies should evaluate whether the results, in particular, the cognitive and sensory preparation can be extended to other more complex tasks such as multiple choice or visual search and different sensory modalities such as auditory and somatosensory.

6. Conclusions

The study showed adult normative ERP data in two visuomotor tasks (SRT and DRT) commonly used in the literature, and in a purely visual task (Passive task). Several novel components in the pre-stimulus (the vN) and post-stimulus (the pN2, the pN3 and the pP3) phases are reported, which add to the other pre-stimulus (the pN) and post-stimulus (the pN1, the Pp1 and the pP2) components, previously found in recent studies using the same visuomotor tasks. The Passive task allowed us to describe for the first time the proactive vN component likely originating in extrastriate visual areas. The vN could reflect a modality-specific form of anticipatory attention, which likely facilitate perceptual processing in visual tasks.

Acknowledgements

The study was supported by the University of Rome “Foro Italico” Rome, Italy and Santa Lucia Foundation (IRCCS Fondazione Santa Lucia), Rome Italy.

Appendix A. Supplementary data

Supplementary data to this article can be found online at https://doi.org/10.1016/j.neuroimage.2019.04.033.

References

Arieli, A., Sterkin, A., Grinvald, A., Aertsen, A.D., 1996. Dynamics of ongoing activity: explanation of the large variability in evoked cortical responses. Science 273 (5283), 1868–1871.

Aron, A.R., Robbins, T.W., Poldrack, R.A., 2004. Inhibition and the right inferior frontal cortex. Trends Cognit. Sci. 8 (4), 170–177.

Berchicci, M., Lucci, G., Pesce, C., Spinelli, D., Di Russo, F., 2012. Prefrontal hyperactivity in older people during motor planning. Neuroimage 62 (3), 1750–1760.

Berchicci, M., Lucci, G., Di Russo, F., 2013. Benefits of physical exercise on the aging brain: the role of the prefrontal cortex. J Gerontol A Biol Sci Med Sci. 68 (11), 1137–1341.

Berchicci, M., Spinelli, D., Di Russo, F., 2016. New insights into old waves. Matching stimulus-and response-locked ERPs on the same time-window. Biol. Psychol. 117, 202–215.

Berchicci, M., Sulpizio, V., Mento, G., Lucci, G., Civale, N., Galati, G., Pitzalis, S., Spinelli, D., Di Russo, F., 2018. Prompting Future Events: Effects of Temporal Cueing and Time on Task on Brain Preparation to Action. Brain Structure and Function (submitted for publication).

Berchicci, M., Ten Brink, A.F., Quinzi, F., Perri, R.L., Spinelli, D., Di Russo, F., 2019. Electrophysiological evidence of sustained spatial attention effects over anterior cortex: possible contribution of the anterior insula. Psychophysiology. https://doi.org/10.1111/psyp.13369 (in press).

Bianco, V., Di Russo, F., Perri, R.L., Berchicci, M., 2016. Different proactive and reactive action control in Fencers' and Boxers' brain. Neuroscience 20, 260–268.

Bianco, V., Berchicci, M., Perri, R.L., Quinzi, F., Di Russo, F., 2017c. Exercise-related cognitive effects on sensory-motor control in athletes and drummers compared to non-athletes and other musicians. Neuroscience 360, 39–47.

Bianco, V., Berchicci, M., Perri, R.L., Spinelli, D., Di Russo, F., 2017b. The proactive self-control of actions: time-course of underlying brain activities. Neuroimage 156, 388–393.

Bianco, V., Di Russo, F., Perri, R.L., Berchicci, M., 2017a. Different proactive and reactive action control in fencers' and boxers' brain. Neuroscience 20, 260–268.

Bogacz, R., Wagenmakers, E.J., Forstmann, B.U., Nieuwenhuis, S., 2010. The neural basis of the speed–accuracy tradeoff. Trends Neurosci. 33 (1), 10–16.

Bozzacchi, C., Giusti, M.A., Pitzalis, S., Spinelli, D., Di Russo, F., 2012. Awareness affects motor planning for goal-oriented actions. Biol. Psychol. 89 (2), 503–514.

Brunia, C.H.M., Van Boxtel, G.J.M., 2004. Anticipatory attention to verbal and non-verbal stimuli is reflected in a modality-specific SPN. Exp. Brain Res. 156 (2), 231–239.

Brunia, C.H., Hackley, S.A., van Boxtel, G.J., Kotani, Y., Ohgami, Y., 2011. Waiting to perceive: reward or punishment? Clin. Neurophysiol. 122 (5), 858–868.

Busch, N.A., VanRullen, R., 2010. Spontaneous EEG oscillations reveal periodic sampling of visual attention. Proc. Natl. Acad. Sci. Unit. States Am. 107 (37), 16048–16053.

Corbetta, M., Patel, G., Shulman, G.L., 2008. The reorienting system of the human brain: from environment to theory of mind. Neuron 58 (3), 306–324.

Craig, A.D., Craig, A.D., 2009. How do you feel–now? The anterior insula and human awareness. Nat. Rev. Neurosci. 10 (1), 59–70.

Cunnington, R., Windischberger, C., Deecke, L., Moser, E., 2002. The preparation and execution of self-initiated and externally-triggered movement: a study of event-related fMRI. Neuroimage 15, 373–385.

Cunnington, R., Windischberger, C., Deecke, L., Moser, E., 2003. The preparation and readiness for voluntary movement: a high-field event-related fMRI study of the Bereitschafts-BOLD response. Neuroimage 20, 404–412.

Delorme, A., Miyakoshi, M., Jung, T.P., Makeig, S., 2015. Grand average ERP-image plotting and statistics: a method for comparing variability in event-related single-trial EEG activities across subjects and conditions. J. Neurosci. Methods 250, 3–6.

Desmedt, J.E., 1980. P300 in serial tasks: an essential post-decision closure mechanism. Prog. Brain Res. 54, 682–686.

Di Russo, F., Pitzalis, S., 2014. EEG-fMRI Combination for the Study of Visual Perception and Spatial Attention. Cognitive Electrophysiology of Attention: Signals of the Mind. Academic Press, London, pp. 58–70.

Di Russo, F., Berchicci, M., Bozzacchi, C., Perri, R.L., Pitzalis, S., Spinelli, D., 2017. Beyond the "bereitschaftspotential": action preparation behind cognitive functions. Neurosci. Biobehav. Rev. 78, 57–81.

Di Russo, F., Lucci, G., Sulpizio, V., Berchicci, M., Spinelli, D., Pitzalis, S., Galati, G., 2016. Spatiotemporal brain mapping during preparation, perception, and action. Neuroimage 126, 1–14.

Di Russo, F., Pitzalis, S., Spitoni, G., Aprile, T., Patria, F., Spinelli, D., Hillyard, S.A., 2005. Identification of the neural sources of the pattern-reversal VEP. Neuroimage 24 (3), 874–886.

Di Russo, F., Stella, A., Spitoni, G., Strappini, F., Sdoia, S., Galati, G., Hillyard, S.A., Pitzalis, S., 2012. Spatiotemporal brain mapping of spatial attention effects on pattern-reversal ERPs. Hum. Brain Mapp. 33 (6), 1334–1351.

Filimon, F., 2010. Human cortical control of hand movements: parietofrontal networks for reaching, grasping and pointing. Neuroscientist 16, 388–407.

Gómez, C.M., Flores, A., Ledesma, A., 2007. Fronto-parietal networks activation during the contingent negative variation period. Brain Res. Bull. 73 (1–3), 40–47.

Gómez, C.M., Marco, J., Grau, C., 2003. Preparatory visuo-motor cortical network of the contingent negative variation estimated by current density. Neuroimage 20 (1), 216–224.

Gonçalves, F.G., Rego, G., Conde, T., Leite, G., Carvalho, S., Lapenta, O.M., Boggio, P.S., 2018. Mind wandering and task-focused attention: ERP correlates. Sci. Rep. 8 (1), 7608.

Griffiths, T.L., Kemp, C., Tenenbaum, J.B., 2008. Bayesian models of cognition. In: Sun, Ron (Ed.), The Cambridge Handbook of Computational Psychology. Cambridge University Press.

Hari, R., Puce, A., 2017. MEG-EEG Primer. Oxford University Press.

Jahanshahi, M., Hallett, M. (Eds.), 2003. The Bereitschaftspotential: Movement-Related Cortical Potentials. Springer Science & Business Media.

Jones, M., Love, B.C., 2011. Bayesian fundamentalism or enlightenment? On the explanatory status and theoretical contributions of Bayesian models of cognition. Behav. Brain Sci. 34 (4), 169–188.

Jung, T.P., Makeig, S., Humphries, C., Lee, T.W., Mckeown, M.J., Iragui, V., Sejnowski, T.J., 2000. Removing electroencephalographic artifacts by blind source separation. Psychophysiology 37 (2), 163–178.

Kamijo, K., Bae, S., Masaki, H., 2016. The association of childhood fitness to proactive and reactive action monitoring. PLoS One 11 (3), e0150691.

Kastner, S., Pinsk, M.A., De Weerd, P., Desimone, R., Ungerleider, L.G., 1999. Increased activity in human visual cortex during directed attention in the absence of visual stimulation. Neuron 22 (4), 751–761.

Knill, D.C., Richards, W. (Eds.), 1996. Perception as Bayesian Inference. Cambridge University Press.

Kornhuber, H.H., Deecke, L., 1965. Changes in the brain potential in voluntary movements and passive movements in man: readiness potential and reafferent potentials. Pflugers Arch. für Gesamte Physiol. Menschen Tiere 284, 1–17.

Linden, D.E., 2005. The P300: where in the brain is it produced and what does it tell us? Neuroscientist 11 (6), 563–576.

Luck, S.J., 2014. An Introduction to the Event-Related Potential Technique. MIT press.

Luck, S.J., Gaspelin, N., 2017. How to get statistically significant effects in any ERP experiment (and why you shouldn't). Psychophysiology 54 (1), 146–157.

Luck, S.J., Kappenman, E.S. (Eds.), 2011. The Oxford Handbook of Event-Related Potential Components. Oxford university press.

Luck, S.J., Heinze, H.J., Mangun, G.R., Hillyard, S.A., 1990. Visual event-related potentials index focused attention within bilateral stimulus arrays. II. Functional dissociation of P1 and N1 components. Electroencephalogr. Clin. Neurophysiol. 75 (6), 528–542.

Mamassian, P., Landy, M., Maloney, L.T., 2002. Bayesian modelling of visual perception. Probabilist. Model Brain 13–36.

Menon, V., Uddin, L.Q., 2010. Saliency, switching, attention and control: a network model of insula function. Brain Struct. Funct. 214 (5–6), 655–667.

Nieuwenhuis, S., Aston-Jones, G., Cohen, J.D., 2005. Decision making, the P3, and the locus coeruleus–norepinephrine system. Psychol. Bull. 131 (4), 510.

Odom, J.V., Bach, M., Barber, C., Brigell, M., Marmor, M.F., Tormene, A.P., Holder, G.E., 2004. Visual evoked potentials standard (2004). Doc. Ophthalmol. 108 (2), 115–123.

Oldfield, R.C., 1971. The assessment and analysis of handedness: the Edinburgh inventory. Neuropsychologia 9 (1), 97–113.

Ouyang, G., Hildebrandt, A., Sommer, W., Zhou, C., 2017. Exploiting the intra-subject latency variability from single-trial event-related potentials in the P3 time range: a review and comparative evaluation of methods. Neurosci. Biobehav. Rev. 75, 1–21.

Pascual-Marqui, R.D., Michel, C.M., Lehmann, D., 1994. Low resolution electromagnetic tomography: a new method for localizing electrical activity in the brain. Int. J. Psychophysiol. 18, 49–65.

Pascual-Marqui, R.D., 2002. Standardized low-resolution brain electromagnetic tomography (sLORETA): technical details. Methods Find Exp. Clin. Pharmacol. 24, 5–12.

Pernet, C., Garrido, M., Gramfort, A., Maurits, N., Michel, C., Pang, E., et al., 2018. Best Practices in Data Analysis and Sharing in Neuroimaging Using MEEG. https://doi.org/10.31219/osf.io/a8dhx10.31219. White paper.

Perri, R.L., Berchicci, M., Bianco, V., Quinzi, F., Spinelli, D., Di Russo, F., 2018b. Awareness of perception and sensory-motor integration: ERPs from the anterior insula. Brain Struct. Funct. 223 (8), 3577–3592.

Perri, R.L., Berchicci, M., Bianco, V., Quinzi, F., Spinelli, D., Di Russo, F., 2019. Perceptual Load in Decision Making: the Role of Anterior Insula and Visual Areas. An ERP Study. Neuropsychologia (in press).

Perri, R.L., Berchicci, M., Bianco, V., Spinelli, D., Di Russo, F., 2018a. Brain waves from an "isolated" cortex: contribution of the anterior insula to cognitive functions. Brain Struct. Funct. 223 (3), 1343–1355.

Perri, R.L., Di Russo, F., 2017. Executive functions and performance variability measured by event-related potentials to understand the neural bases of perceptual decision-making. Front. Hum. Neurosci. 11, 556.

Perri, R.L., Berchicci, M., Lucci, G., Cimmino, R.L., Bello, A., Di Russo, F., 2014a. Getting ready for an emotion: specific premotor brain activities for self-administered emotional pictures. Front. Behav. Neurosci. 8.

Perri, R.L., Berchicci, M., Lucci, G., Spinelli, D., Di Russo, F., 2015. The premotor role of the prefrontal cortex in response consistency. Neuropsychology 29 (5), 767.

Perri, R.L., Spinelli, D., Di Russo, F., 2017. Missing the target: the neural processing underlying the omission error. Brain Topogr. 30 (3), 352–363.

Perri, R.L., Berchicci, M., Spinelli, D., Di Russo, F., 2014b. Individual differences in response speed and accuracy are associated to specific brain activities of two interacting systems. Front. Behav. Neurosci. 8, 251.

Perri, R.L., Berchicci, M., Lucci, G., Spinelli, D., Di Russo, F., 2016. How the brain prevents a second error in a perceptual decision-making task. Sci. Rep. 6, 32058.

Pitzalis, S., Strappini, F., Bultrini, A., Di Russo, F., 2018. Detailed spatiotemporal brain mapping of chromatic vision combining high-resolution VEP with fMRI and retinotopy. Hum. Brain Mapp. 39 (7), 2868–2886.
Polich, J., 2007. Updating P300: an integrative theory of P3a and P3b. Clin. Neurophysiol. 118, 2128–2148.
Potts, G.F., Liotti, M., Tucker, D.M., Posner, M.I., 1996. Frontal and inferior temporal cortical activity in visual target detection: evidence from high spatially sampled event-related potentials. Brain Topogr. 9 (1), 3–14.
Puce, A., Hämäläinen, M., 2017. A review of issues related to data acquisition and analysis in EEG/MEG studies. Brain Sci. 7 (6), 58.
Quinzi, F., Perri, R.L., Berchicci, M., Bianco, V., Spinelli, D., Di Russo, F., 2018. The independency of the Bereitschaftspotential from previous stimulus locked P3 in visuo-motor response tasks. Psychophysiology, e13296 (in press).
Ragazzoni, A., Di Russo, F., Fabbri, S., Pesaresi, I., Di Rollo, A., Perri, R.L., Barloscio, D., Bocci, T., Cosottini, M., Sartucci, F., 2019. "Hit the missing stimulus". A simultaneous EEG-fMRI study to localize the generators of endogenous ERPs in an omitted target paradigm. Sci. Rep. 9 (1), 3684.
Sanchez-Lopez, J., Pedersini, C.A., Di Russo, F., Cardobi, N., Fonte, C., Varalta, V., Prior, M., Smania, N., Savazzi, S., Marzi, C.A., 2017. Visually evoked responses from the blind field of hemianopic patients. Neuropsychologia. https://doi.org/10.1016/j.neuropsychologia.2017.10.008 (in press).
Shibasaki, H., Hallett, M., 2006. What is the Bereitschaftspotential? Clin. Neurophysiol. 117 (11), 2341–2356.
Spironelli, C., Busenello, J., Angrilli, A., 2016. Supine posture inhibits cortical activity: evidence from Delta and Alpha EEG bands. Neuropsychologia 89, 125–131.
Sterzer, P., Kleinschmidt, A., 2010. Anterior insula activations in perceptual paradigms: often observed but barely understood. Brain Struct. Funct. 214 (5–6), 611–622.
Sulpizio, V., Lucci, G., Berchicci, M., Galati, G., Pitzalis, S., Di Russo, F., 2017. Hemispheric asymmetries in the transition from action preparation to execution. Neuroimage 148, 390–402.
Thut, G., Nietzel, A., Brandt, S.A., Pascual-Leone, A., 2006. α-Band electroencephalographic activity over occipital cortex indexes visuospatial attention bias and predicts visual target detection. J. Neurosci. 26 (37), 9494–9502.
van Boxtel, G.J., Böcker, K.B., 2004. Cortical measures of anticipation. J. Psychophysiol. 18 (2/3), 61–76.
Verleger, R., Baur, N., Metzner, M.F., Smigasiewicz, K., 2014. The hard oddball: effects of difficult response selection on stimulus-related P3 and on response-related negative potentials. Psychophysiology 51, 1089–1100.
Wiech, K., Lin, C.S., Brodersen, K.H., Bingel, U., Ploner, M., Tracey, I., 2010. Anterior insula integrates information about salience into perceptual decisions about pain. J. Neurosci. 30 (48), 16324–16331.